

BRIGHTON/ YOUNG UNIVERSITY

GEOLOGY STUDIES

VOLUME 25 PART 1

DECEMBER 1981

Brigham Young University Geology Studies

Volume 28, Part 3

CONTENTS

Three Creeks Caldera, Southern Pavant Range, Utah	Thomas A. Steven
Biostratigraphy of the Great Blue Formation	Alan K. Chamberlain
Carbonate Petrology and Depositional Environments of the Sinbad Limestone Member of the Moenkopi Formation in the Teasdale Dome Area, Wayne and Garfield Counties, Utah	James Scott Dean
Geology of the Antelope Peak Area of the Southern San Francisco Mountains, Beaver County, Utah	Vince L. Felt
The Tintic Quartzite in Rock Canyon, Utah County, Utah: A Model for Shallow-shelf Sedimentation	Craig D. Hall
Geology of the Longlick and White Mountain Area, Southern San Francisco Mountains	Dan E. Haymond
Geology of the Auburn 7½' Quadrangle, Caribou County, Idaho, and Lincoln County, Wyoming	David E. Jenkins
Carbonate Petrology and Depositional Environments of the Limestone Member of the Carmel Formation, near Carmel Junction, Kane County, Utah	Douglas W. Taylor



Cover: Slab of bivalves showing Myalina-Pleuroma suite, from Torrey section, Sinbad Limestone Member, Moenkopi Formation in the Teasdale Dome Area, Wayne County, Utah. Photo courtesy James Scott Dean.

A publication of the
Department of Geology
Brigham Young University
Provo, Utah 84602

Editors

W. Kenneth Hamblin
Cynthia M. Gardner

Brigham Young University Geology Studies is published by the Department of Geology. This publication consists of graduate student and faculty research within the department as well as papers submitted by outside contributors. Each article submitted by BYU faculty and outside contributors is externally reviewed by at least two qualified persons.

ISSN 0068-1016

Distributed December 1981

12-81 600 52593

CONTENTS

Three Creeks Caldera, Southern Pavant Range, Utah, by Thomas A. Steven	1	Carbonate Petrology and Depositional Environments of the Sinbad Limestone Member of the Moenkopi Formation in the Teasdale Dome Area, Wayne and Garfield Counties, Utah, by James Scott Dean	19
Abstract	1	Abstract	19
Introduction	1	Introduction	19
Regional setting	2	Location	19
Three Creeks Tuff Member	2	Methods and terminology	20
Evolution of the Three Creeks Caldera	4	Field methods	20
Comparisons	5	Laboratory methods	20
References	7	Terminology	20
Figures		Previous work	22
1. Geologic map	1	Geologic setting	22
2. Distribution of Three Creeks Tuff Member	2	Acknowledgments	23
3. View into subsided block of caldera	3	Geometry and petrology of carbonate lithofacies	23
4. View of topographic wall	4	Lithofacies A	23
5. Interpreted relations	4	Stromatolitic boundstone subfacies	24
6. Talus-landslide breccia	5	Oolite-peloid packstone subfacies	25
7. Talus breccia along topographic wall of caldera	6	Dolomicrite subfacies	26
8. Grooves on topographic wall of caldera	6	Channel conglomerate subfacies	26
9. Ternary diagram	7	Evaporite subfacies	26
Biostratigraphy of the Great Blue Formation, by Alan K. Chamberlain	9	Lithofacies B	28
Introduction	9	Skeletal packstone subfacies	28
Location and purpose	9	Pellertal wackestone subfacies	30
Previous work	9	Lithofacies C	30
Fieldwork	9	Lithofacies D	33
Laboratory work	9	Oolite-mollusk packstone subfacies	33
Depositional environment of the Great Blue Formation	9	Peloidal mudstone-wackestone subfacies	34
Acknowledgments	10	Lithofacies E	34
Stratigraphic sections	10	Lithofacies F	36
Oquirrh Mountain section (1)	10	Correlation of lithofacies	36
Onaqui Mountain section (2)	10	Paleontology	37
Ochre Mountain section (3)	11	Ichnology	37
Boulter Peak (4)	11	Diagenesis	37
Wasatch Mountain section (5)	12	Recrystallization	38
Wellsville Mountain section (6)	12	Dolomitization	38
Fossils	14	Homogeneous dolomites	38
Conodonts	14	Heterogeneous dolomites	38
Corals	14	Depositional environments of carbonate lithofacies	39
Brachiopods	14	Lithofacies A	39
Bryozoans	14	Stromatolitic boundstone subfacies	39
Sponge	14	Oolite-peloid packstone subfacies	40
Cephalopods	16	Dolomicrite subfacies	41
Plants	16	Channel conglomerate subfacies	41
Other fossils	16	Evaporite subfacies	41
Conclusion	16	Lithofacies B	41
References cited	17	Lithofacies C	42
Figures		Lithofacies D	42
1. Index map	9	Lithofacies E	42
2. Oquirrh Mountain (section 1)	10	Lithofacies F	43
3. Onaqui Mountain (section 2)	11	Depositional summary	43
4. Ochre Mountain (section 3)	12	Petroleum potential	44
5. Boulter Peak (section 4)	13	Potential of lithofacies	45
6. Wasatch Mountains (section 5)	13	Appendix	45
7. Wellsville Mountain (section 6)	14	References cited	45
8. East-west correlation	16	Figures	
Table		1. Index map	19
1. First and last occurrences of organisms in the Great Blue Formation	15	2. Outcrop of Sinbad Limestone Member	20
		3. Fence diagram: stratigraphic relationships	21

4. Stratigraphic sections in pocket	Needles Range Formation	54
5. Classification of carbonate rocks 21	Wah Wah Springs Tuff Member	55
6. A.—Paleotectonic features 23	Lund Tuff Member	55
B.—Paleogeography and sedimentary facies 23	Wallaces Peak Tuff Member	55
7. Photomicrograph: stromatolitic boundstone 24	Isom Formation	55
8. Slab showing cryptalgal dolomicrite 24	Formation of Blawn Wash	55
9. Photomicrograph: recrystallized packstone fabric 25	Tuff Member of Sevey's Well	55
10. Photomicrograph: packstone from Torrey section 25	Quartz Latite Member of Squaw Peak	56
11. Photomicrograph: cryptalgal dolomicrite 26	Lower tuff member	56
12. A.—High-angle cross-bedding 27	Sandstone member	57
B.—Carbonate flaser bedding 27	Upper tuff member	57
C.—Channel conglomerate 27	Rhyolite flow member	57
D.—Cryptalgal dolomicrite 27	Lava flow member	57
E.—Herringbone cross-bedding 27	Basaltic conglomerate	57
F.—Herringbone cross-sets 27	Basalt flow	57
13. Flat-pebble and subrounded intraclasts 28	Lower conglomerate	58
14. Rippled and gypsiferous dolomicrite 28	Upper conglomerate	58
15. A.—Cyclic bioturbation 29	Alluvium	58
B.—Tidal channel 29	Structure	58
C.—Skeletal packstone 29	General statement	58
D.—Tidal channel 29	Northeast-trending faults	58
E.—Planar cross-bedding 29	Northwest-trending faults	58
F.—Massive pygmatic gypsum 29	East-trending faults	59
16. Photomicrograph: massive gypsum 30	Eruptive centers	59
17. Photomicrograph: pelletal wackestone 30	Age of faulting	59
18. Photomicrograph: grainstone layer 30	Oligocene to early Miocene faulting	59
19. Photomicrograph: umbrella structure 30	Mid-Miocene faulting	59
20. Photomicrograph: <i>Skolithos</i> burrow filled with debris 31	Post mid-Miocene basin-and-range faulting	60
21. Photomicrograph: mollusk wackestone 31	Summary	60
22. A.—View of Grand Wash section 32	Geologic history	60
B.—Contact between claystone and shales 32	Early Tertiary to middle Oligocene	60
C.—Teepee ridges 32	Middle Oligocene to late Oligocene	60
D.—Ripple marks 32	Early Miocene to Recent	60
E.—Limestones held up by channeled dolomites 32	Miocene depression	62
23. Photomicrograph: remnant lamination in dolomite .. 33	Alteration	63
24. Photomicrograph: recrystallized skeletal packstone .. 33	Conclusions	64
25. Photomicrograph: dissolution surface, packstone and wackestone 34	References	65
26. Sinbad Limestone Member 34	Figures	
27. Photomicrograph: heterogeneous dolomite 35	1. Index map of the Antelope Peak area	53
28. Photomicrograph: dolomitized oolite grainstone 35	2. Correlation of map units	55
29. Photomicrograph: dolomite fabric 35	3. Tuff Member of Sevey's Well	56
30. Photomicrograph: dolomitized peloids 35	4. Quartz Latite Member of Squaw Peak showing typical spheroidal weathering and popcorn texture	56
31. View of tidal channel 36	5. Photomicrograph (crossed nicols): Quartz Latite Member of Squaw Peak	56
32. Diagram: relationships of depositional environments 40	6. Photomicrograph (crossed nicols): xenocrysts of subhedral plagioclase enclosed in a reaction rim	57
33. A.—Transgressing tidal flat-sabka 43	7. Photomicrograph (crossed nicols): felted matrix of plagioclase microlites in the basalt flow unit	58
B.—Subtidal deposition of second phase 43	8. Map of fault patterns and intensely altered rocks	59
C.—Final phase of deposition 43	9. Diagrammatic cross section, illustrating the concept of northeast-striking subordinate listric faults	59
Plates	10. Regional geologic map	61
1. Ammonoids, gastropods, bivalves 49	11. Gravity map, southern San Francisco Mountains	62
2. Bioturbation, sponge, spicule net 51	12. Autoclastic breccia unit, Quartz Latite Member of Squaw Peak	63
Geology of the Antelope Peak Area of the Southern San Francisco Mountains, Beaver County, Utah, by Vince L. Felt 53	13. Approximate location of Miocene depression	63
Introduction 53	14. Magnetic map	64
Objectives 53	Plate	
Location 53	1. Geologic map of the Antelope Peak area in pocket	
Previous work 54		
Geologic setting 54	The Tintic Quartzite in Rock Canyon, Utah County, Utah: A Model for Shallow-shelf Sedimentation, by Craig D. Hall 67	
Acknowledgments 54		
Stratigraphy 54		
General statement 54		
Dacite of Shauntie Hills 54		

Introduction	67	Toroweap Formation	86
Location of study area	67	Kaibab Limestone	87
Methods of study	67	Jurassic System	87
Previous work	68	Navajo Sandstone	87
Acknowledgments	68	Tertiary System	87
Lithology	68	Dacite of Shauntie Hills	87
Sedimentary structures	69	Needles Range Formation	87
Biogenic sedimentary structures	69	Wah Wah Springs Tuff Member	88
Interpretation	69	Lund Tuff Member	88
Cross-bedding analysis	71	Wallaces Peak Tuff Member	88
Vertical successions	72	Isom Formation	88
Deposition of the Tintic Quartzite	75	Hole-in-the-Wall Tuff Member	88
Other examples of clastic sedimentation	75	Formation of Blawn Wash	88
Shallow-shelf sedimentation	76	Tuff of Sevey's Well Member	88
Summary	77	Quartz Latite of Squaw Peak Member	88
References cited	79	Lower tuff member	88
Figures		Mafic flow member	89
1. Index map of study sections	67	Upper tuff member	89
2. Block diagram of planar cross-bedding	69	Rhyolite flow member	89
3. Block diagram of trough cross-bedding	70	Formation of Brimstone Reservoir	89
4. Block diagram of channel features	71	Alluvial cover	89
5. Steampower graph	71	Structure	89
6. Velocity vs. grain size graph	72	General statement	89
7. Average current directions in the formation	73	Thrust faults	89
8. Columnar sections of the Tintic Quartzite	74	East-west-trending faults	89
9. Columnar sections of the Flathead Sandstone	76	North-south-trending faults	90
10. Columnar section of the Duolbasgaissa Formation, Norway	77	Northeast-southwest-trending faults	90
11. Idealized vertical sequence of shallow-shelf, transgressive deposits	79	Northwest-southeast-trending faults	90
Table		Folds	90
1. Special fluid depth-velocity quantities and their respective Froude Numbers	70	Alteration	90
		Mineralization	91
		Geologic history	91
		Economic potential	94
		Appendix	94
		References cited	99
		Figures	
		1. Index map	81
		2. Composite Paleozoic section	82
		3. Paleozoic correlation diagram	84
		4. Great Blue Limestone at White Mountain	85
		5. Overturned section of Pakoon Formation and Callville Limestone	86
		6. Toroweap and Kaibab Limestone at Miners Hill	87
		7. Aerial view of the Brimstone Lineament	90
		8. Monocline in the Humbug Formation	91
		9. Hydrothermal bleaching along a joint	92
		10. Silicified upper tuff member	92
		11. Brimstone sinter mound	93
		12. Fumarole lined with native sulfur	93
		Plate	
		1. Geology of the Longlick and White Mountain area ..	in pocket
Geology of the Longlick and White Mountain Area, Southern San Francisco Mountains, by Dan E. Haymond	81		
Abstract	81		
Introduction	81		
Location	81		
Previous work	81		
Acknowledgments	81		
Stratigraphy	82		
General statement	82		
Devonian System	83		
Sevy Dolomite	83		
Guilmette-Simonson Dolomite	83		
Cove Fort Quartzite	83		
Crystal Pass Limestone	83		
Pinyon Peak Limestone	83		
Mississippian System	83		
Monte Cristo Limestone	83		
Dawn-Whitmore Wash Limestone Member ..	83		
Anchor-Thunder Springs Limestone Member ..	83		
Deseret Limestone	85		
Humbug Formation	85		
Great Blue Limestone	85		
Chainman Shale	86		
Pennsylvanian System	86		
Callville Limestone	86		
Permian System	86		
Pakoon Limestone	86		
Queantoweap Sandstone	86		
		Geology of the Auburn 7½' Quadrangle, Caribou County, Idaho, and Lincoln County, Wyoming, by David E. Jenkins	101
		Introduction	101
		Previous work	101
		Method of study	101
		Acknowledgments	101
		Stratigraphy	102
		General statement	102
		Permian System	102
		Phosphoria Formation	102
		Rex Chert Member	102

Triassic System	102	Plate	
Dinwoody Formation	102	1. Geologic map of the Auburn Quadrangle	in pocket
Woodside Formation	103		
Thaynes Formation	103	Carbonate Petrology and Depositional Environments	
A member	103	of the Limestone Member of the Carmel Formation,	
B member	104	near Carmel Junction, Kane County, Utah, by	
Portneuf Limestone Member	104	Douglas W. Taylor	117
Lower member of the Thaynes Formation	104	Abstract	117
Upper member of the Thaynes Formation	104	Introduction and geologic setting	117
Ankareh Formation	104	Location	118
Lanes Tongue of the Ankareh Formation	104	Methods of study and nomenclature	118
Wood Shale Tongue of the Ankareh		Previous work	118
Formation	104	Acknowledgments	119
Ankareh Formation of the Absaroka Plate	104	Geometry and petrology of lithofacies	119
Higham Grit	104	Lithofacies A	119
Jurassic System	105	Lithofacies B	119
Nugget Sandstone	105	Siltstone subfacies	119
Twin Creek Limestone	105	Dolomicrite subfacies	119
Preuss Sandstone	105	Stromatolitic boundstone subfacies	119
Stump Sandstone	106	Evaporite dolomicrite subfacies	120
Cretaceous System	106	Lithofacies C	121
Ephraim Conglomerate	107	Oolite skeletal packstone and grainstone	
Peterson Limestone	107	subfacies	121
Bechler Conglomerate	107	Bivalve wackestone subfacies	121
Draney Limestone	107	Lithofacies D	122
Tygee Member of the Bear River Formation	107	Lithofacies E	122
Wayan Formation	108	Lithofacies F	123
Tertiary System	108	Peloidal grainstone subfacies	124
Salt Lake Formation	108	Stromatolitic boundstone subfacies	124
Quaternary System	108	Correlation	125
Structure	108	Paleontology	125
General statement	108	Ichnology	126
Meade Thrust Fault	109	Diagenesis	126
Faults	109	Recrystallization	126
Tear faults	109	Dolomitization	127
Transverse faults	109	Depositional environments of lithofacies	127
North-south high-angle faults	109	Lithofacies A	127
Folds	109	Lithofacies B	128
Economic geology	111	Dolomicrite subfacies	128
Petroleum	111	Stromatolitic boundstone subfacies	128
Phosphate	112	Evaporite subfacies	129
Hot springs	112	Lithofacies C	129
Other deposits	112	Lithofacies D	129
Summary	112	Lithofacies E	129
Appendix	112	Lithofacies F	129
References	116	Depositional summary	129
Figures		Petroleum potential	131
1. Index map	101	Appendix	131
2. Generalized stratigraphic column	102	References cited	133
3. Rex Chert Member of the Phosphoria Formation	103	Figures	
4. Member divisions Thaynes-Ankareh Formations	103	1. Index map	117
5. Ammonites of the Thaynes Formation	104	2. Paleogeographic map	118
6. Twin Creek Limestone	105	3. Carmel Limestone Member	118
7. Twin Creek Limestone	106	4. Nine measured sections	in pocket
8. Ripple marks, Stump Sandstone	106	5. Photomicrograph: dolomitic siltstone subfacies	120
9. Ripple marks, Stump Sandstone	107	6. Photomicrograph: thinly bedded dolomicrite	120
10. Slickensides, Ephraim Conglomerate	107	7. Cryptalgal bedding	120
11. Tygee Member of the Bear River Formation	108	8. Photomicrograph: stromatolitic boundstone	120
12. Salt Lake Formation	108	9. Photomicrograph: nodular anhydrite and dolomi-	
13. Salt Springs Stump Valley	108	cite	121
14. Thrust fault zones, Idaho-Wyoming	110	10. Cross-bedded oolite-skeletal packstone	121
15. Imbrication of footwall	111	11. Drawing: possible bryozoan colony	121
16. Spring Creek Syncline	112	12. Photomicrograph: oolite-skeletal packstone	122
17. Active hot springs	112	13. Encrinal grainstone	122

14. Weathered surface of packstone	122	22. Photomicrograph: peloidal grainstone	126
15. Echinoid spines	122	23. Ripple marks in dolomicrite	126
16. (A) <i>Diademopsis</i> , (B) <i>Ostrea</i> (<i>Liostrea</i>) <i>strigulecula</i> , (C) <i>Gryphaea</i> valve, (D) <i>Cossmannia imlayi</i> , (E) <i>Lima</i> (<i>Plagiostoma</i>) <i>zonja</i> valve, (F) possible cyclostome bryozoan colony, (G) coelenterate ? colony, (H) <i>Lima</i> (<i>Plagiostoma</i>) <i>occidentalis</i> valve, (I) <i>Mesenteripora</i> encrusting <i>Ostrea</i> shell	123	24. Photomicrograph: packstone	126
17. Photomicrograph: wackestone subfacies	124	25. Photomicrograph: partially recrystallized oolites	127
18. Wackestone subfacies	124	26. Depositional model for the Carmel Limestone Member	128
19. Units exposed in roadcut	124	27. Ripple marks	130
20. Photomicrographs: (A) argillaceous mudstone and (B) micro-cross-bedding	125	28. Bivalve coquina	130
21. Photomicrograph: peloidal grainstone	126	29. Transgressive oolite shoals, phase I; regression of sea and prograding shale, phase II; minor transgression of peloidal grainstones, phase III	130
		30. Generalized stratigraphic column	131
		Publications and maps of the Geology Department	135

The Tintic Quartzite in Rock Canyon, Utah County, Utah: A Model for Shallow-Shelf Sedimentation*

CRAIG D. HALL
Gulf Research and Development Company
P.O. Box 36506
Houston, Texas 77036

ABSTRACT.—The vertical sequence of rock types and primary sedimentary structures in the Tintic Quartzite of Rock Canyon, Utah, forms the basis for a model of shallow-shelf sedimentation. The lower 10 m of the formation is a quartz-gravel conglomerate set in a medium to coarse quartz sand matrix. The remainder of the unit is a well-sorted, fine-grained quartzite. Vertical successions of primary sedimentary structures include horizontal bedding, planar and trough cross-bedding, and ripple-bedding. The Tintic Quartzite is predominantly a horizontally bedded quartzite with occasional cross-bedded units that are more common near the base. These units commonly show a well-preserved sequence of trough cross-bedding and ripple-bedding overlain by horizontal bedding. The horizontal bedding is interpreted to be a product of the lower flow regime because of the conformable contact commonly found between it and underlying ripple-bedding.

The Tintic Quartzite in Rock Canyon was deposited in a nearshore marine environment, worked initially by longshore currents. In later stages, sediment transport was offshore into deeper water, where fluctuations in current velocity were less frequent.

By a comparison of the Tintic Quartzite with the Flathead Sandstone of western Wyoming, an idealized vertical sequence of rock types and sedimentary structures is constructed. The basal portion of the sequence will typically be a conglomerate with grain sizes ranging from medium-grained sand to small boulders. Overlying the conglomerate will be an upward fining sequence of medium- to fine-grained quartz sand. Sedimentary structures show an upward trend of decreasing flow velocity and more consistent current directions.

INTRODUCTION

The Tintic Quartzite of central Utah is an excellent example of a basal clastic unit in a marine transgressive sequence. It is well exposed throughout the Wasatch Mountains and is easily accessible. It is important because it records the first of several Paleozoic transgressions that moved across the continent. There appear to be no major unconformities in the formation, and it is thus a more or less complete sequence in which to study the results of sedimentary processes that took place in a shallow marine setting.

This study documents the vertical succession of sedimentary structures and rock types in the Tintic Quartzite in Rock Canyon, Utah County, Utah. The vertical succession provides the basis for deriving a model for shallow marine sedimentation that will be restricted to shallow marine basal transgressive deposits of mature quartzose sandstone and is not meant to explain or predict sequences in carbonate- or mud-dominated shelf deposits. The model is intended to provide a clearer understanding of the processes operating on the shelf during the deposition of these rocks from interpretation of the bedforms that generated the vertical succession of sedimentary structures.

Location of Study Area

Three sections of the Tintic Quartzite in the Wasatch Mountains that were originally along depositional strike (Lochman-Balk 1971) were selected for this study. The Rock Canyon section is located at the mouth of Rock Canyon, 2 km northeast of Provo, Utah. Here the Tintic is exposed in an asymmetrical anticlinal fold with the axial plane dipping to the west.

The section is a composite from exposures on both the north and south walls of the canyon.

Supplementary sections are located on the south wall of American Fork Canyon in the Timpanogos Cave National Monument 20 km northwest of Rock Canyon, and on Y Mountain 1.5 km south of Rock Canyon. Both sections are well exposed but are faulted, and portions of each are obscured (fig. 1).

Methods of Study

The Rock Canyon section was photographed in approximately 30-m intervals from the far side of the canyon from each interval. These photos were used as base maps on which were recorded the vertical succession of sedimentary structures.

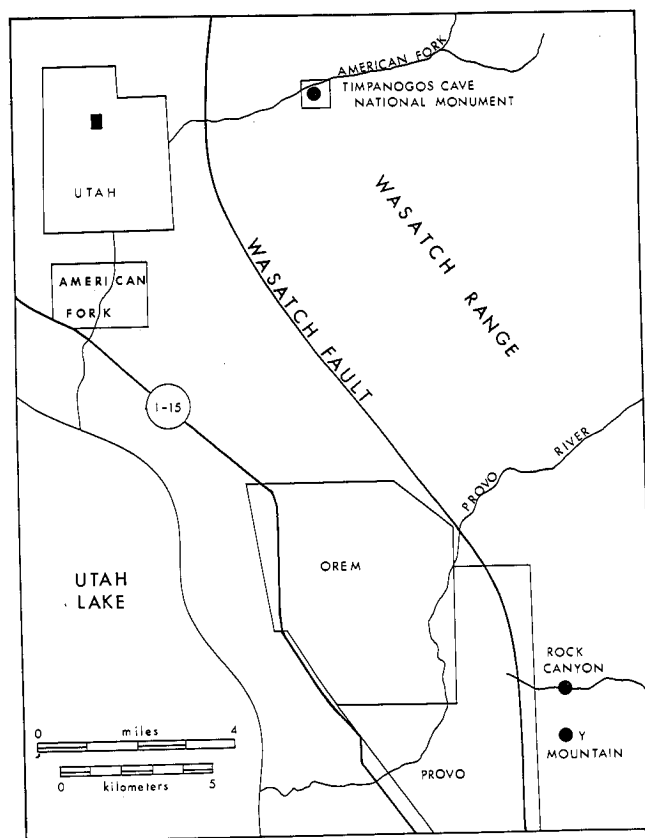


FIGURE 1.—Index map. Circles show locations of sections of the Tintic Quartzite discussed in this report.

*A thesis presented to the Department of Geology, Brigham Young University, in partial fulfillment of the requirements for the degree Master of Science, August 1980. Thesis chairman: W. K. Hamblin.

The section was also measured to determine the overall formational and bedding dimensions. The objective was to study in detail the lithologies and vertical successions of the sedimentary structures.

The supplementary sections were photographed or measured. The American Fork section was not photographed because it was impossible to stand back from the canyon wall, but it was measured in detail. Data were collected on lithology, and type and size of sedimentary structures. The Y Mountain section was not measured because the formation formed hazardous cliffs, but was photographed from points along strike of the bedding.

The data on the three sections were then compiled into columnar sections to study the vertical succession of sedimentary structures. These structures were used to interpret their generating bedforms, and the model proposed here was developed to explain their vertical occurrences.

Previous Work

Since the term *Tintic Quartzite* was first applied by Smith (1900) to basal Paleozoic clastics in the Tintic district, numerous workers have labored to define the formation in terms of areal extent, general characteristics, and stratigraphic relationships. Eardley and Hatch (1940) defined its northward extent and reported general rock types within the formation. Eardley (1944) measured a section of the Tintic, along with other Cambrian rocks, in Ogden Canyon. He gave a rough outline of the unit in terms of rock types but did not mention any sedimentary structures. A more detailed description was given for the Tintic of Slate Canyon by Gwynn (1948). He reported an apparent lava flow in the Tintic about 55 m above the base and mentioned differences in the unit above and below the flow. He made mention of the rock below the flow having a "lensy" character to it and being rather poorly sorted. Above the flow, Gwynn reported that the formation was better sorted and thinly bedded.

The overall stratigraphic relationships of the Tintic Quartzite have been studied by Maxey (1958). He postulated a source area to the northwest for the late Early Cambrian rocks and outlined the geometry of the formation over much of western Utah. Lochman-Balk (1959, 1971, 1976) correlated the Cambrian rocks of the Tintic mining district to the lowest Paleozoic rocks in the western Uinta Mountain area and presented panel diagrams (1959) showing the relationships. Morris and Lovering (1961) redefined the Tintic type section in the Tintic District and presented a rough outline of vertical lithologic variation throughout the formation.

To date the Tintic Quartzite has not been examined on a detailed basis to determine its actual step-by-step deposition. This prior work has been critical in establishing a good regional framework for this study.

Detailed facies analysis of stratigraphic equivalents of the Tintic Quartzite include work done by Oriel and Armstrong (1971) on the Brigham Quartzite and by Hereford (1977) in the Tapeats Sandstone. Using detailed biostratigraphy and cross sections Oriel and Armstrong constructed lithofacies maps for northern Utah for each Lower and Middle Cambrian trilobite zone. Hereford (1977) separated the Tapeats Sandstone of central Arizona into six facies. This separation was based on grain-size trends, trace-fossil assemblages, sedimentary structures, and dispersion of cross-bed azimuths.

Acknowledgments

This study is an outgrowth of one made in the Flathead Sandstone of Western Wyoming in 1974 under the direction

of Roger D. Hoggan and Glenn F. Embree of Ricks College. Since 1975, I have received assistance and invaluable help from Steven S. Oriel and David Seeland of the U.S. Geological Survey in Denver, Christina Lochman-Balk of the New Mexico Institute of Mining and Technology, and fellow graduate students of Brigham Young University. W. Kenneth Hamblin and J. Keith Rigby of Brigham Young University have been instrumental in helping me define and refine the goals of this study. My wife, through it all, has been patient and supportive and kept our lives organized in the midst of chaos.

To each of these people, and anyone else who has offered me assistance, I express a heartfelt thank you.

LITHOLOGY

In Rock Canyon the Tintic Quartzite is a moderately well sorted quartzite. Grain sizes range from 0.7- or 0.8-mm sand grains to 4-cm cobbles of quartz. Only trace amounts of feldspar and lithic fragments were found. The cobbles are found near the base of the section below the 30-m level, and above that the largest grains are 1.0 mm in diameter. The sand grains are well cemented with silica, and it has been reported that some well-rounded quartz grains have quartz overgrowths in optical continuity with them (Eardley 1944). For the most part the cement is clear, giving the rock a light tan color, but occasionally iron is present either in reduced or oxidized states, giving a green or red tint, respectively, to the rock. Other than quartz, euhedral hematite crystals are the only mineral found, and they occur in a green colored quartzite at the 26-m level.

In the American Fork section the formation is composed of moderately to poorly sorted quartz pebbles and sand. The base is inaccessible, but in the lower 4 m that were measured the rock is a quartz gravel conglomerate with a quartz sand matrix. The gravels are segregated into the laminations of the primary sedimentary structures. The remainder of the formation here is made of moderately well sorted quartz sand except for an interval between 101 and 112 m above the exposed base that has poorly sorted quartz gravels and quartz sands. Through this interval the mean grain size decreases upward to medium sand and remains constant from 112 m to the top of the formation at 126 m. Clear silica is the cement, and only occasionally is it colored or tinted by iron. Again, quartz is the main constituent, with any other minerals making up only trace amounts.

The Y Mountain section is similar to the Rock Canyon section in its grain-size range except in the 9- to 14-m interval. Here quartz cobbles are common in a green quartzite matrix. They show some segregation into large primary sedimentary structure laminations. The interval from 14 to 299 m is moderately sorted quartz sand, with grain sizes from 0.8 to 2.0 mm. A fining upward sequence of quartz gravel and quartz sand extends for 3 m upward from 299 m. From there to the top of the section at 334 m the formation is well-sorted, medium-grained quartz sand. Clear silica and silica stained with varying concentrations of reduced and oxidized iron cements the entire sequence.

In central Utah the Tintic Quartzite forms an eastward-thinning wedge between any two given time-horizons. The isopachs in figure 7 show thicknesses of the formation for the Lower Cambrian. The Rock Canyon section is shown on the 164-m (500-ft) line although in fact it is more than 370 m thick. With continued sedimentation into Middle Cambrian time, additional sediment was deposited which increased the thickness of the section. All three sections show evidence of minor faulting. Deletion of section along these faults together

with possible relief on the early Cambrian topography could explain the discrepancies in thickness among the three sections.

SEDIMENTARY STRUCTURES

Three types of primary sedimentary structures predominate in the Tintic Quartzite. Horizontal bedding is the most common type in the Rock Canyon and Y Mountain sections, but two styles of cross-stratification make up a large portion of the American Fork section and a part of the Rock Canyon section.

Horizontal laminations occur in beds from 1.0 to 90 cm thick that pinch out laterally in 10 to 20 m. The laminations are expressed by alternations of iron-stained silica with clear silica. They are well sorted, and the typical grain size is 1.0 mm. Trough and planar cross-bedding constitute the next most abundant structures. Planar cross-beds show both tangential and angular foreset bases, and in one case, tangential foreset tops and bases. The third type of structure found are channellike features that show asymmetrical internal bedding and are discordant to the bedding around them.

All of these structures range over a broad spectrum of sizes and for purposes of description are divided into three classes: small scale, medium scale, and large scale.

Dimensions of the small-scale sedimentary structures are defined at less than 10 cm vertically and less than 50 cm horizontally. This size range includes small ripple bedding, trough-type cross-bedding, and some planar-type cross-bedding with tangential foreset bases. The ripple-bedding is restricted to heights less than 5 cm and, in some instances, could have been confused with small trough-type owing to poor expression of laminae.

The medium-scale sedimentary structures are from 10 to 50 cm in vertical dimension and from 0.5 to 2 m in horizontal dimension. The dominant structure is planar cross-bedding with both angular and tangential foreset bases. Channel features fit in this size range, as do some larger trough cross-beds that may be near the original size of those trough-shaped structures described above. Trough cross-bedding which is approximately 10 cm high and 4 cm wide may be erosional remnants of these larger structures.

Sedimentary structures from 0.5 to 2 m high and 2 to 20 m wide are here considered to be large scale. They are almost wholly planar-type cross-bedding with tangential foreset bases. In the American Fork section there is large-scale cross-bedding with tangential foreset tops as well as bases. The sets are up to 15 m long and are slightly wedge shaped with undulatory upper and lower contacts. The small- and medium-scale planar cross-bedding discussed above could be erosional remnants of these larger structures.

Biogenic Sedimentary Structures

At the contact between the Tintic Quartzite and Ophir Shale in Rock Canyon are some burrowlike features, similar to *Skolithos* burrows, filled in by red and maroon hematite. The sand around the burrows shows no bedding traces and seems to have been disturbed possibly during activity of the organisms responsible for the burrows.

No other fossils were found in any of the three sections studied for this report. Lochman-Balk (1976) reports that "no fossils have been reported from the Tintic Quartzite in the central Wasatch exposures, (but) cephalia and other fragments identifiable as *Olenellus* sp. have been found in upper beds . . . in the Mt. Nebo area." She also states that *Olenellus* sp. has been found in upper beds of the Brigham Quartzite in the northern Wasatch Range.

Interpretation

Vertical successions of distinctive types of sedimentary structures and associated rock types yield the most important information regarding the genesis of the Tintic Quartzite. These structures reflect the bedforms that created them, which, in turn, reflect the dynamics of the transporting system in operation during the time of deposition. According to Walther's Law, vertical variations in these structures reflect horizontal variations in bedforms in the depositional environment (Walther 1894).

The various primary sedimentary structures found in the Tintic Quartzite were generated by migrating bedforms with specific shapes and dimensions. Planar cross-bedding is attributed to the downcurrent migration of relatively straight-crested sandwaves (Reineck and Singh 1975) (fig. 2). The sandwaves can vary in height from 0.5 cm to 15 m and in length from 0.6 to 1000 m.

Figure 2 is an idealized diagram showing the type of sandwave responsible for the production of planar cross-bedding. These so-called straight-crested ripples will have some sinuosity to them at some point along their length, but for the most part they are linear features. The side panels are based on observed types of cross-bedding in the Tintic and show a typical vertical sequence in outcrop. This type of cross-bedding commonly overlies horizontally bedded quartzite and underlies trough cross-bedding and ripple-bedding.

Trough and festoon cross-bedding is produced during the downcurrent migration of very sinuous, or lunate, sandwaves (Reineck and Singh 1975) (fig. 3). These ripples can vary in size as much as the straight-crested ripples, and the shape of the cross-bed sets can be extremely variable when observed from various angles in cross section. Figure 3 shows a type of sandwave that produced the trough cross-bedding, and at a smaller scale, the ripple-bedding. The transverse cross section shows the shape of the trough cross-bedding found in the Tintic Quartzite. The longitudinal section shows the "planar" cross-bedding with tangential foreset bases generated by these lunate sandwaves. It is possible to find tangential foreset basal contacts in straight-crested sandwaves, but they are largely due to a fine-grained fraction of the sediment being carried over the crest of the ripple and settling through the current shadow to the base. Because of the well-sorted nature of the Tintic, the tangential based foresets are here interpreted as being the product of these lunate, or sinuous, sandwaves.

The channellike features discussed under Sedimentary Structures are similar to those mentioned by Reineck and

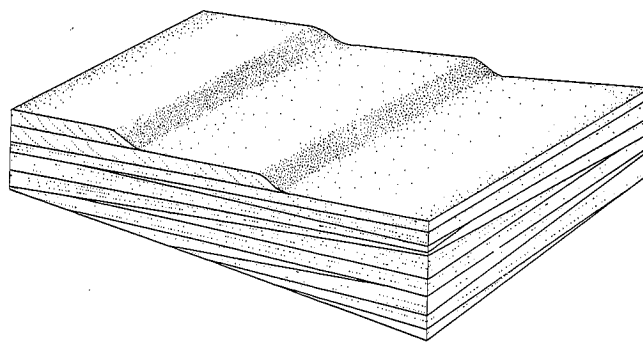


FIGURE 2.—Block diagram illustrating the development of the planar cross-bedding found in the Tintic Quartzite. Side panels are idealized from vertical sequences observed in the Rock Canyon section.

Singh (1975, p. 63) as being the product of subaqueous channel erosion and deposition. In a cross section normal to current flow, the channel would show symmetrical bedding, concave upward. Four of these channels were observed, and in three the bedding shows varying degrees of asymmetry, and one is nearly symmetrical. If a channel with symmetrical bedding is cut at various angles oblique to the current direction it will show varying degrees of asymmetry (fig. 4).

Key factors in determining bedform development are velocity and depth of the transporting medium and grain size of the sediment. The Froude number is a useful quantity to aid in visualizing the dynamics of a flowing medium. It provides limits to interpreting sediment transport mechanics that might otherwise get out of hand. The Froude number (F) is related to velocity, gravity, and depth as shown in the equation

$$F = \frac{V}{\sqrt{gh}}$$

where V is flow velocity, g is the acceleration due to gravity, and h is the depth of the flow. Values of F less than 1 characterize a tranquil-flow regime for the respective fluid velocity and depth. Values greater than 1 delimit a high-flow regime with distinctive bedforms. A predictable evolution of bedforms results as F increases in value from 0 to 1, and from 1 to some upper limit determined by sediment density, beyond which the sediment is held in suspension.

Figure 5 illustrates the various bedforms produced as a function of grain size and streampower (Vt_0). Streampower is a quantity to describe the transporting ability of a moving fluid, where V is the current velocity, and t_0 is a composite quantity of specific weight of the fluid and sediment multiplied by fluid depth and the slope of the energy gradient.

The transition zone shown is where the Froude number is approximately 1 and the lower and upper flow regime is defined at values for F less than 1 and greater than 1, respectively.

As the Froude number increases, the bedforms evolve from small-scale ripples, 0.04 to 0.06 m long and up to 0.06 m high, and planar beds (with increasing grain size), to straight and sinuous large-scale sandwaves from 0.6 to 30 m long, and 0.06 to 1.5 m high. At a point where the Froude number approximately equals 1, the lower-flow regime bedforms are erased, and bedforms of the upper-flow regime develop.

In this study, the upper-flow regime will not be discussed in detail. The reason for this is shown in table 1. For water depths in the shallow marine environment (5 to 100 m), current velocities must be approximately 7 to 30 m per second to yield a Froude number equal to 1. Current velocities even 3 m per second are extremely rare and generated for short periods of time during storms or in narrow tidal bores. Generally velocities are less than 2 m per second and consequently produce Froude numbers from 0.3 to 0.06.

Using figure 5 and plotting the average grain size in the Tintic Quartzite (0.8 to 1.0 mm) with the various bedforms represented by the observed sedimentary structures, a more or less smooth trend is seen from planar bedding to large-scale sandwaves of varying degrees of sinuosity. This trend may reflect either increasing current velocity or increasing water depth.

Table 1

Water depth(m)	Current velocity (m/sec)	Froude number
0.01	0.31	1
0.1	0.99	1
1.0	3.12	1
10	9.9	1
100	31.32	1

TABLE 1.—Summary of current velocities required to generate Froude numbers equal to 1 for varying flow depths.

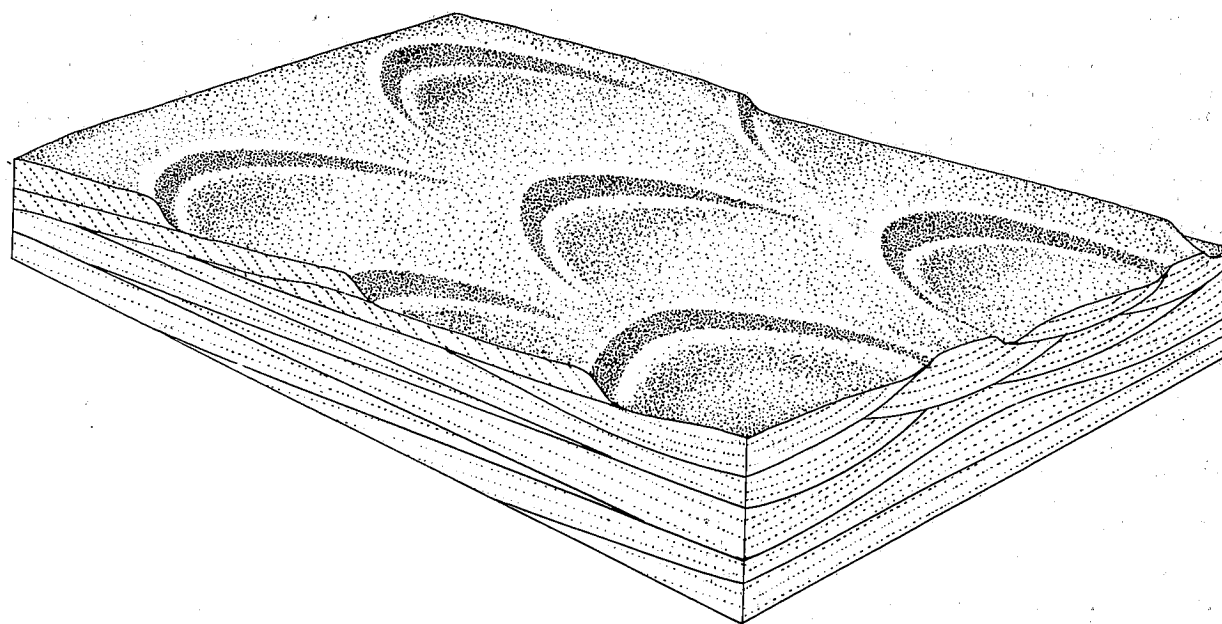


FIGURE 3.—Block diagram illustrating the development of the trough cross-bedding found in the Tintic Quartzite. Side panels are idealized from vertical sequences observed in the Rock Canyon section.

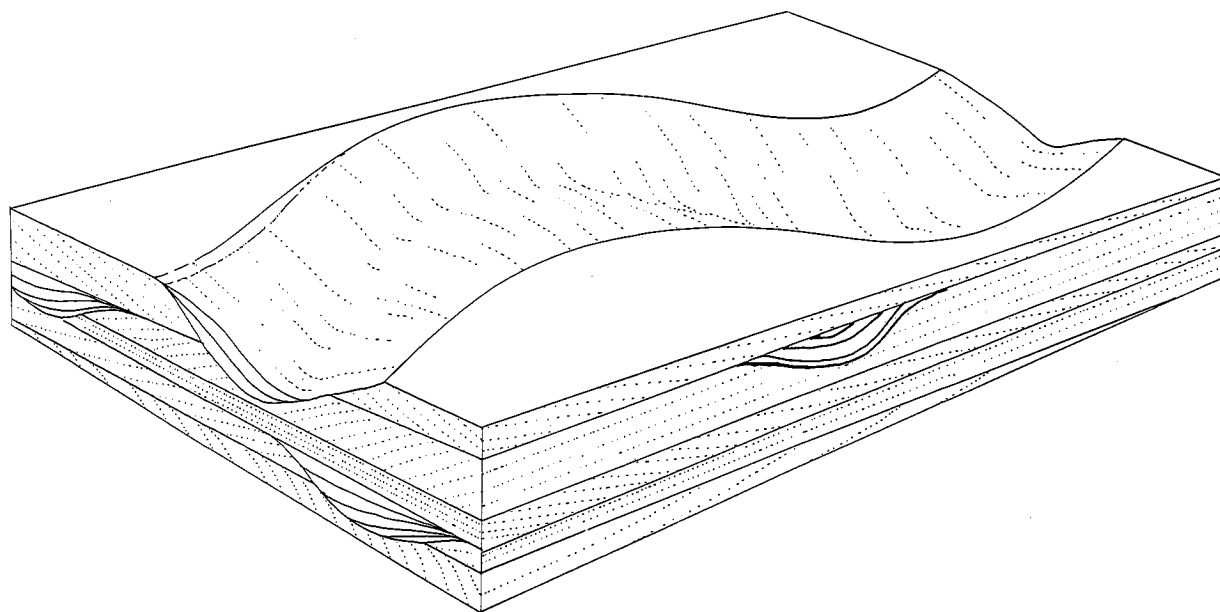


FIGURE 4.—Block diagram illustrating the interpretation of the channel-features found in the basal Tintic. The side panels show the observed structures from the Tintic, and the upper face shows the interpreted feature.

Figure 6 shows the relationship between grain size and current velocity and various bedforms in an attempt to illustrate what velocities might be represented by the various bedforms. The data for this came from experiments involving a water depth of 0.2 m (Southard 1971). For greater water depths the velocities would need to be slightly greater. In order to maintain the same Froude number at 2.0 m of water depth, the velocity must be increased by a factor of 3. At 2.0 m of water depth, the planar beds shown at 0.5 m per second would be generated at 1.5 m per second. Southard (1971) said that "since lower (planar) bed states are associated with low sediment transport rates, parallel lamination in coarse sands is probably much more commonly the record of upper (planar)-bed states." But Guy and others (1966) and Liu (1957) reported plane beds with significant sediment movement at low flow velocities. With such a large vertical sequence of planar beds in the Tintic Quartzite representing long periods of consistent deposition and the limits of the Froude number discussed above, the planar beds of the Tintic Quartzite are interpreted to be a product of the lower-flow regime.

With increasing current velocity, the planar beds evolve through straight-crested ripples showing angular foreset bases, to more and more sinuous ripples. This transition is documented in the Tintic Quartzite by the vertical sequences of planar bedding, small-scale ripple-bedding, festoon and tabular cross-bedding, and medium- and large-scale festoon and tabular cross-bedding.

CROSS-BEDDING ANALYSIS

Cross-bed dip directions were measured and compiled as part of this study to determine paleocurrent directions in the Tintic Quartzite and the variability of those directions through time. These quantities can be determined statistically, and the grouping of measurements vertically provides a look at changes in the direction of sediment transport through time. The value of such studies is twofold. First, ancient patterns of sediment movement can be compared to patterns in various modern dep-

ositional environments and a closer and clearer comparison made. Second, paleographic changes, such as transgressing or regressing coastline or the development of irregularities along the coastline, may be reflected in a change in current patterns.

A total of 78 cross-bed dip direction measurements were taken in the Rock Canyon section. These were packaged into

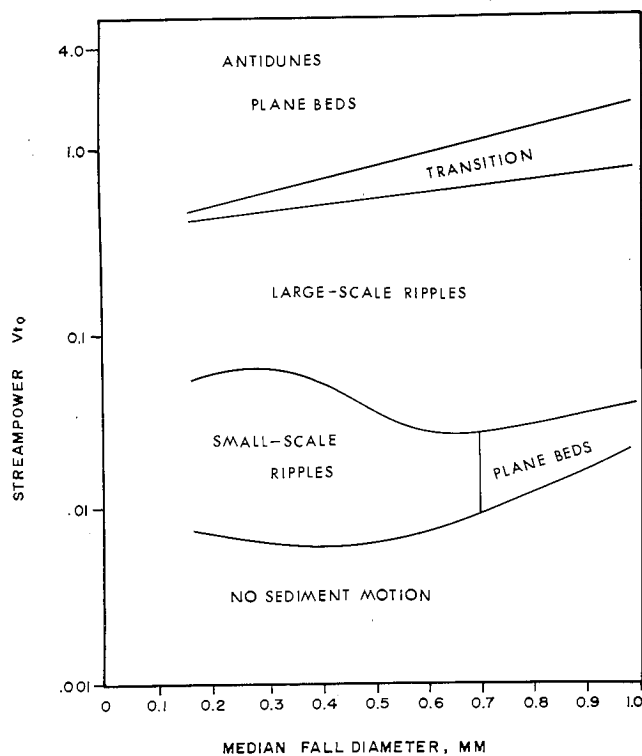


FIGURE 5.—Relation of stream power and median fall diameter to bedform types.

three groups. The lowest group was from 0 to 60 m in the section, the middle group from 60 to 300 m, and the upper from 300 to 377 m. They were taken, for the most part, on lineations of stained cement or alternations of varying grain sizes. These are the most common expressions of cross-bedding rather than exposed foreset faces because the formation is too firmly cemented to allow much etching or separation along laminae. These measurements were trend and plunge attitudes that had to be converted on an equal area net to true dip, and then the true dip measurements from the field were added to them. The nearly vertical tilt of the enclosing beds was removed, and dip directions were then transferred to circular histograms.

The most useful evaluation to define average direction of sediment dispersal is that of mean cross-bed dip direction. This is best done using methods outlined by Pincus (1956) and Curray (1956). The compass direction of mean cross-bed dip direction or average current direction, is given by

$$\tan \Theta = \frac{\sum n \sin \theta}{\sum n \cos \theta}$$

where Θ is the vector resultant bearing, θ the midpoint of each 10-degree azimuth cell on the histogram, and n is the total number of readings in each cell.

Another useful quantity in analyzing directional data is standard deviation

$$S\Theta = \frac{\sum (\Theta - \theta)^2}{(\sum n) - 1}$$

where $S\Theta$ is the standard deviation in degrees, $(\Theta - \theta)$ is the difference between each cell midpoint in degrees and the bearing of the vector resultant in degrees, and $\sum n$ is the total number of measurements. This quantity is important in better understanding the variability of current direction.

The results of these calculations are shown in figure 7. Figure 7a shows the average current direction by the arrow and standard deviation by the fan for the lower Tintic Quartzite. The compass direction of the arrow is calculated at 124° , or to the southeast with a standard deviation of 37° . The broad standard deviation is a result of a strong southerly component on the histogram that is overwhelmed on the average current direction. When these data are overlain on the isopachs of the Tintic as shown in figure 7a, the average current direction is approximately 45° from the trend of the isopachs in an on-shore direction. Figure 7b shows the average current direction for the middle portion of the formation along with its 24° standard deviation. The mean direction is 204° to the southwest, but the strongest component on the histogram is at about 245° , or more westerly. There are a few measurements to the southeast that bring the average more easterly, but the narrower standard deviation shows the more dominant south-westerly direction. Figure 7c shows a mean current direction of 255° for the upper portion of the Tintic. This came from a polymodal histogram with the two strongest components roughly parallel to the sides of the standard deviation fan. These two components probably represent measurements on arcuate sandwave slip faces.

The distinct change in current directions between the base and top of the formation from southeast to almost due west shows the development of an offshore component of current direction out from an originally longshore-onshore direction. The mechanism to induce the offshore currents is not clear, but the pattern is documented in the cross-bed dip directions and orientation with regard to the shoreline as has been shown in figure 7.

This offshore transport pattern has been noted in other shallow-shelf clastic sequences. Hamblin (1961) found in the Franconia Formation of the Lake Superior region paleocurrent directions indicating sediment transport away from the zero isopach line into the thicker isopachs. Hall (1975) reported paleocurrent directions of the Flathead Sandstone of the Teton Mountains showing net sediment transport to the southwest normal to the isopach lines for the formation. Seeland (1969) gathered cross-bed dip directions from the basal Cambrian and Ordovician clastic deposits of North America. When they are correlated with general Cambrian isopachs, the same offshore trend exists.

VERTICAL SUCCESSIONS

Figure 8 illustrates the vertical successions of the sedimentary structures and rock types in the Tintic Quartzite in American Fork Canyon, in Rock Canyon, and on Y Mountain. These patterns are the basis for interpretation of the deposition of the formation.

In the American Fork section the lowest 14 m are covered and inaccessible. When the beds of this interval were observed elsewhere, they are similar to those found in the 14- to 18-m interval. The rock is a well-indurated, quartz-gravel conglomerate set in a medium sand matrix. Primary sedimentary

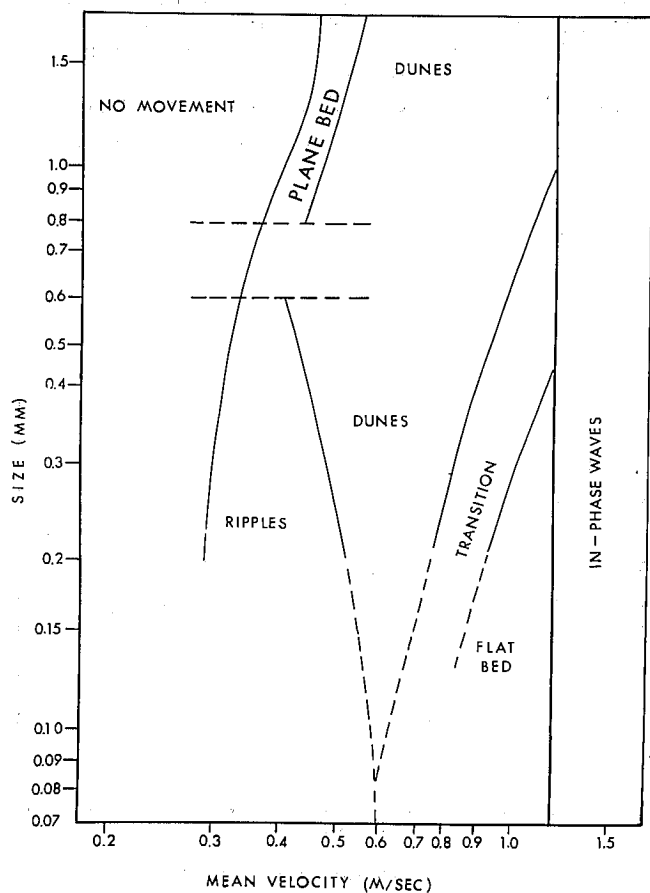


FIGURE 6.—Size-velocity diagram for 0.2-m flow depth showing bedforms produced.

structures include medium-scaled trough cross-bedding and occasional horizontal bedding. The structures are expressed by alternations of gravel and sand-sized particles that have been segregated into the layers.

From 18 to 102 m the rock is a medium-grained quartz sand. There are no gravel-sized fragments, and the grains are well indurated with clear silica. Where the sedimentary structures are observable, they are mostly medium-scale planar cross-beds with occasional trough cross-bedding and horizontal bedding. The upper half of this interval tends to have more horizontal bedding than the lower half, though, with grain size remaining constant.

The interval from 102 to 112 m is quite similar to the lower 14- to 18-m interval. Quartz gravels appear at numerous horizons, associated with scour features and medium-scale trough cross-bedding. Included in the interval are 2 sets of large planar cross-beds with tangential foreset tops and bases, discussed under large-scale sedimentary structures. Between these two sets is a 0.3-m interval of coarse-grained gravels in small-scale trough cross-bedding. In the upper 7 m of this interval the grain sizes decrease upwards to 112 m, where the rock is well sorted and is made up of 0.8- to 1.0-mm-sized quartz grains. This sequence is dominated by medium-scale planar cross-beds occasionally expressed by faint iron staining along foreset laminations.

The remaining 14 m of section is a well-sorted quartzite with occasional thin lenses of green shale similar to the overlying Ophir Shale. Planar cross-bedding predominates in this interval. Horizontal bedding is rare and usually occurs in thin wedges between thick cosets of cross-bedded quartzite.

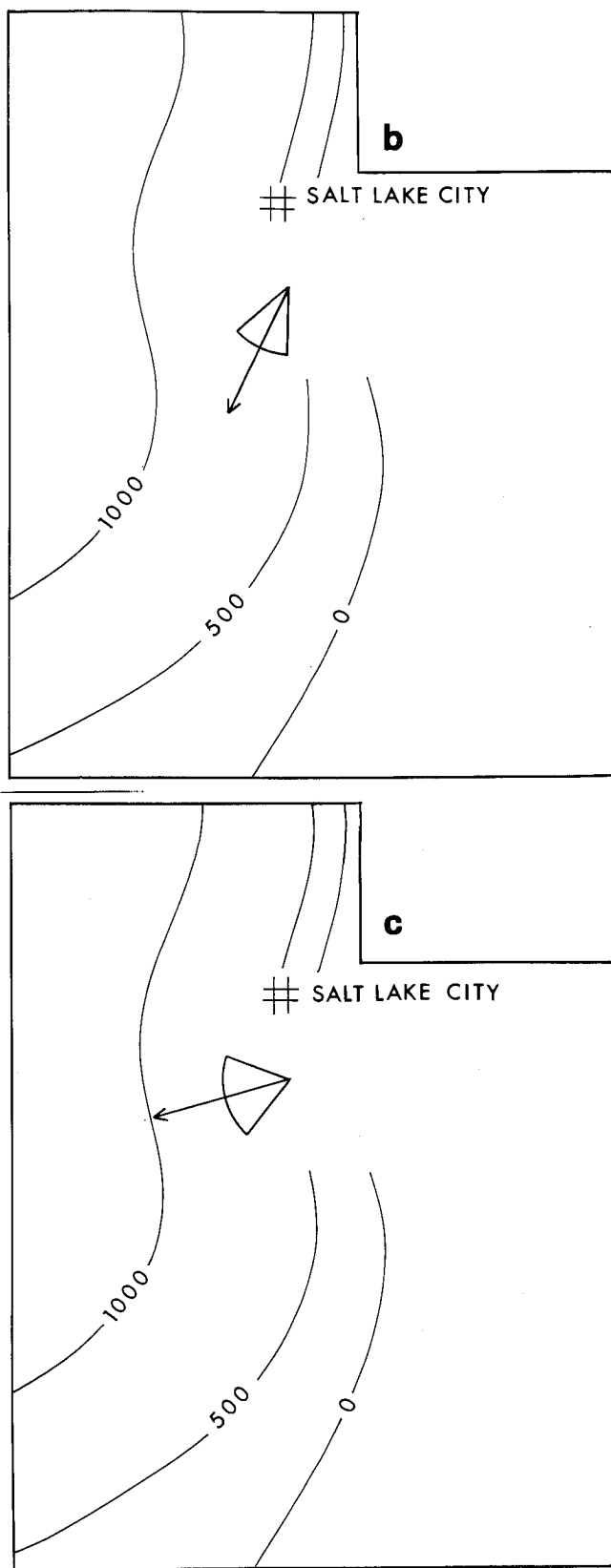


FIGURE 7.—Average current directions and standard deviation for *a*, the lower portion of the formation; *b*, the middle portion; and *c*, the upper portion with respect to the isopachs for the Lower Cambrian. Isopachs shown are in feet.

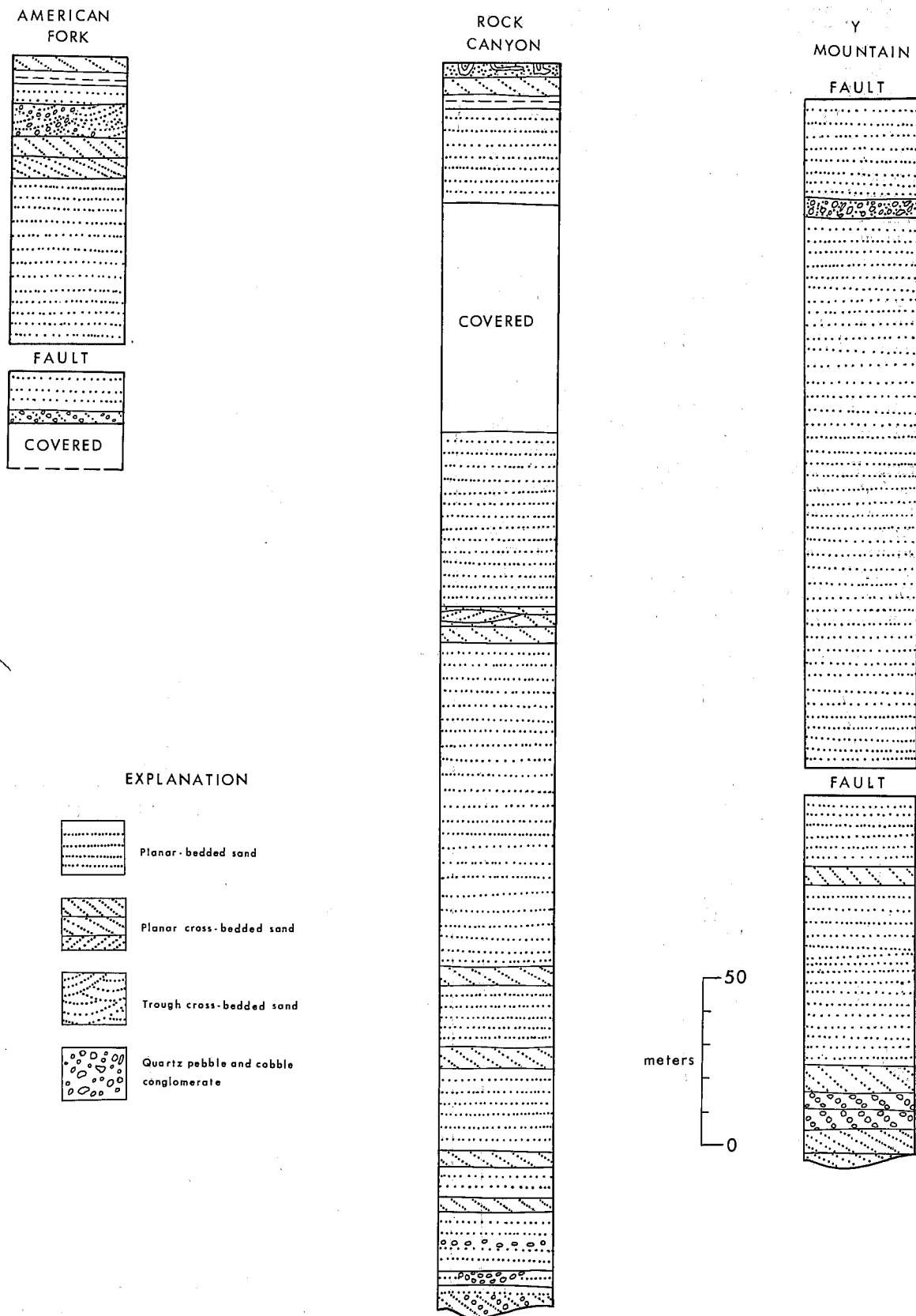


FIGURE 8.—Vertical successions of primary sedimentary structures in the American Fork, Rock Canyon, and Y Mountain sections of the Tintic Quartzite.

The Rock Canyon section is a somewhat simpler section and is divided into four intervals. The basal interval from 0 to 10 m is a quartz cobble and gravel conglomerate set in a matrix of medium- to coarse-grained quartz sand, and the stratification of the sedimentary structures is expressed by alternations of these grains. No lithic fragments or feldspars were found in this basal unit. It is compositionally very mature in contrast to other basal Cambrian rocks, such as the Deadwood Formation in the Black Hills area (Ladle 1972), the Flathead Sandstone of Wyoming (Hall 1975), and the Brigham Quartzite of northern Utah (Oriol and Armstrong 1971). In Rock Canyon the sedimentary structures for this interval include medium-scale trough and planar cross-bedding. The channel features discussed in Sedimentary Structures are present in this interval and are unique to it. They are discordant and are separated, both vertically and laterally, by horizontally bedded, and trough and planar cross-bed sets. They are generally made of coarser-grained material than the enclosing beds.

The interval from 10 to 373 m is a monotonous sequence of horizontally bedded, medium-grained quartzite, with only occasional cross-bedded or ripple-bedded strata. Except for a covered interval from 270 to 340 m the rocks are well exposed on the south side of Rock Canyon. Grain size does not vary throughout the interval and remains at 0.6 to 1.0 mm. The degree of cementation does not vary, and the few cross-bedded intervals are similar in appearance. They are characterized by medium-scaled trough and planar cross-bedding overlain by ripple-bedded quartzite. There is no sharp, straight contact between the ripple-bedded intervals and the overlying horizontal beds. Were this horizontally layered quartzite a product of the upper flow regime, one would expect to find a sharp, eroded contact showing truncation of the upper segments of any cross-bedding. Instead there is a gradual change in structures, more or less well preserved, from medium-scale trough to small-scale planar cross-bedding to ripple-bedding to horizontal bedding with no change in grain size.

The interval from 373 to 377 m shows large-scale planar cross-bedded quartzite with tangential bases and thin lenses of horizontally bedded quartzite. Grain size is in the 0.6- to 0.7-mm range. Lenses of green shale similar to the overlying Ophir Shale are irregularly interbedded with the quartzite. The uppermost set of planar cross-bedding is also at the upper contact and shows bioturbation. The cross-bed laminations are expressed by alternations of purple iron-stained silica with clear silica.

On Y Mountain a slightly different section is seen. From 0 to 9 m the formation is a white, well-sorted, medium-grained quartzite. It shows medium-scale trough cross-bedding. Above this, from 9 to 14 m, is a conglomeratic unit made of quartz cobbles and quartz pebbles set in a dark green quartz sand matrix. The cobbles and pebbles are segregated into the laminations of large-scale trough cross-bedding. The contact with the lower unit is abrupt and undulatory, and within the conglomerate are several undulatory horizons that truncate the upper segments of the cross-bed laminations below them.

Another change in lithology and structure is seen at the 14-m level. From 14 m to the top of the section at 334 m the rock is quite similar to that in Rock Canyon. It is well-sorted with continuous grain size, cemented by clear silica and is predominantly horizontally bedded. As in Rock Canyon there are occasional cross-bedded sets through this interval. They are similarly associated with ripple-bedding and overlain by horizontal bedding.

At 289 m a 1.5- to 2.0-m interval of quartz-pebble con-

glomerate occurs. Sedimentary structures in it are not well defined, either by segregation of grain size or by colored cement, and may be lacking altogether.

DEPOSITION OF THE TINTIC QUARTZITE

Stage I: During the initial deposition of the Tintic Quartzite, the sediments were transported by currents paralleling the shoreline. Alternations of cross-bedded and horizontally bedded quartzite, along with the conglomeratic material at the base, indicate that currents were variable and strong but not strong enough to completely rework the conglomeratic beach deposits. These rocks probably represent very shallow water deposition where the sediment was subject to storm-induced current surges.

Stage II: The bulk of the formation was deposited in a low-energy environment not as susceptible to the frequent surges in current velocity as was the lower basal unit in stage I. Water depth increased steadily, as reflected in the less frequent occurrence of higher-velocity sedimentary structures toward the top of the unit. The constant grain size vertically through the unit probably reflects a texturally mature source sediment. In other basal clastic sequences a steady decrease in grain size from bottom to top has been noticed (Hall 1975).

In the Rock Canyon area the Tintic Quartzite is compositionally, as well as texturally, mature. This maturity, along with the white quartzite at the base of the Y Mountain section, may indicate a previously existing quartzose sandstone unit that provided the sediment for the Tintic. Underlying the American Fork section is the Precambrian Mutual Formation which is a red to maroon quartzite. However, the Mutual is overlain by the Mineral Fork Tillite in Rock Canyon, but it may be an example of such a rock unit that could have been exposed elsewhere prior to the deposition of the Tintic.

Though near the end of deposition the sediment was protected from frequent current surges by deeper water, there were occasions when high-velocity conditions did prevail, possibly during minor regressions or during intense storms. Gravels near the top of the unit and large-scale cross-bedding indicate that conditions were still such as to allow exceptional high-velocity currents to work the sediments into large ripples for brief periods of time and to transport gravel-sized material.

The lack of fossils in the Tintic may be due to unfavorable conditions for preservation in the turbulent water. The fragmentary nature of the fossils that are found attests to high-energy conditions over the substrate.

OTHER EXAMPLES OF CLASTIC SEDIMENTATION

The Tintic Quartzite is one example of clastic deposition in a shallow marine shelf environment. In contrast to sequences interpreted as tidal flat deposits with large quantities of shale and silt (Banks 1973), the Tintic is made up almost wholly of medium-grained sand with only minor amounts of shale.

The Flathead Sandstone of western Wyoming (Hall 1975) is another basal clastic unit almost devoid of shale or mud (fig. 9). It differs from the Tintic in its feldspar content, grain-size trend, and types of sedimentary structures. At its base the Flathead is arkosic with almost 50% feldspar and 50% quartz, in a matrix of red ferruginous clay. The feldspar content decreases vertically up through the unit to only trace amounts at the top. At the top the rocks are well cemented by clear silica. Grain size also decreases vertically through the Flathead, from quartz-cobbles at the base to fine quartz sand at the top.

Medium-scale wedge-shaped, planar cross-stratification is the dominant sedimentary structure in the Flathead. In con-

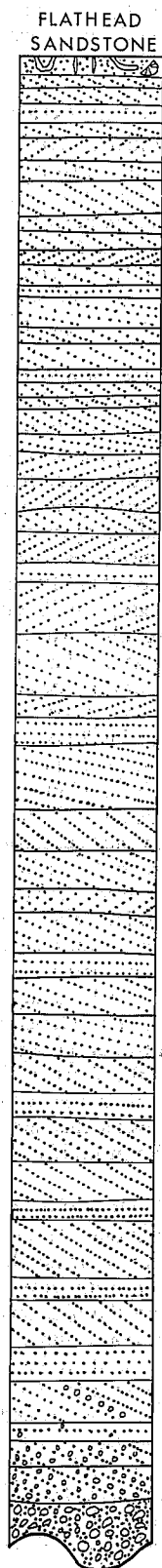


FIGURE 9.—Vertical succession of sedimentary structures in the Flathead Sandstone of western Wyoming. Biogenic material at top includes burrows and brachiopods.

trast to the Tintic Quartzite of Rock Canyon in which horizontal bedding predominates, the Flathead shows only subordinate sets of horizontal bedding in the lower portion. These beds are typically made of coarser-grained sediments and are less well sorted than the sand in the cross-bedded sets above and below them. Upper segments of cross-bedded foresets appear to be truncated and overlain by these horizontal beds. These horizontal beds are interpreted to be the product of high-velocity, upper-flow regime conditions. Such flow conditions indicate shallow water less than 1 m deep. In the upper portion of the section, horizontal bedding is absent and small-scale cross-stratification is dominant. Increasing water depth produced a decrease in energy, and well-differentiated sediments were transported into deeper, quieter water.

The Duolbasgaissa Formation of northern Norway (Banks 1973) is a basal Cambrian transgressive sequence that is somewhat different from either the Tintic Quartzite or the Flathead Sandstone (fig. 10). It is a vertical sequence of mudstone and siltstone showing very small-scale cross-bedding and ripple marks overlain by a mature quartzose sandstone with large-scale cross-bedding. Paleocurrent directions in the sandstones show almost a universal bimodal tendency normal to the paleoshoreline. Banks interprets the unit as a tidal-flat environment. The muds and fine-grained sediments were deposited on nearshore tidal flats that were periodically subaerially exposed, and the sandstones represent offshore, tidal-flat sand bars.

These three sections illustrate two different water-depth and current-energy realms on the shelf: low-energy shelves in which currents are generated by tidal action, and high-energy shelves where current energy is generated by wave action. These two concepts are not new, but they are extremely important considerations when attempting to interpret vertical sequences of quartz sand deposits.

SHALLOW-SHELF SEDIMENTATION

The model proposed here for shallow-shelf sedimentation is based on the Tintic Quartzite of Rock Canyon and supported by information from sections of the Tintic near Rock Canyon, and the Flathead Sandstone section of western Wyoming. It is restricted to sediments being deposited in a sublittoral, high-energy environment above effective wave base. This model assumes a large influx of terrigenous sediments that are transported and sorted on the shelf in increasing water depth. Beach deposits may develop but are usually reworked by wave action during transgression.

A related model was proposed by Irwin (1965) for "clear-water sedimentation." The model assumes no influx of terrigenous clastics and proposes separate environments in an epicontinental sea. Each environment exists in a belt parallel to the shoreline and is separated by the line formed by the intersection of effective wave base and the seafloor. Below this line is the quiet-water shale environment; above are carbonate sands; and shoreward, or leeward, of this belt is a quiet-water zone of lagoons, carbonates, and evaporites extending to the shoreline. This model was developed for the Paleozoic carbonates of the Williston Basin.

The model presented in this paper proposes that during initial stages of deposition the sediment being delivered to the shelf area is made up of quartz sand and cobbles (fig. 11). The primary source of energy is most likely wave action generated by onshore winds. Cobbles and other sediments found at the base of various formations attest to a high-energy regime during this stage I period of deposition. Cobble-conglomerates may be found in ponds in topographic lows in the underlying

rock as wave erosion would incompletely plane a rugged landscape and rework the cobble-sized debris. Tidal currents during this shallow stage will produce bimodal cross-beds.

As the shoreline migrates inland, the water depth over a given point will increase. Longshore currents generated by waves approaching the shoreline obliquely will transport sediment parallel to the shore. This action will be documented by sedimentary structures becoming more typical of quieter water and paleocurrent directions parallel to isopachs of the unit.

Grain size will decrease steadily from the high-energy basal conglomerates to medium-grained sand with deepening water provided that sediment with a broad size range is supplied. If the sediment being delivered is a well-sorted, mature sand, the resulting rock will be mature regardless of the time or distance of transport.

Any fluctuation in current velocity will be documented in the changes in the types of primary sedimentary structures. Horizontal bedding can record either low- or high-velocity flow regimes, and can be separated on the basis of its vertical relationships with underlying and overlying structures. Cross-bedding will record a midrange of current velocity values. Planar cross-bedding reflects migration of straight-crested sandwaves and, with increasing velocity, the crest will become more and more sinuous until trough-shaped cross-beds are produced just before velocity exceeds a critical point, and the bedforms are erased. Size of the primary sedimentary structures can be misleading as subsequent partial erosion of the sandwave may reduce the total thickness to only a fraction of its original value.

SUMMARY

The Tintic Quartzite of Rock Canyon in central Utah is a very mature quartzite cemented wholly by silica. The entire section shows variation only in vertical changes in sedimentary structure types. An understanding of the conditions under which the sediments were deposited can be gained from a hydrodynamic interpretation of the primary sedimentary structures and their vertical succession.

The formation was initially deposited and worked by fluctuating currents that moved the sediment onshore and longshore. Gravels at the base may represent storm deposits or remnants of a beach that was transgressed and reworked. The bulk of the unit was deposited under increasingly quieter conditions with very steady, low-velocity currents that transported the sand offshore.

According to other workers, the shoreline during the deposition of the Tintic generally migrated eastward. If sediment supply to the area was sufficient, water depth may not have increased significantly so the improved sorting of the sediment upsection and the record of steadier currents may reflect increasing distance from the surf zone. Medium-scale cross-bedding at the contact with the Ophir Shale indicates water depth shallow enough to allow wave base, possibly during major storms, to reach bottom.

The Flathead Sandstone in western Wyoming is another basal Paleozoic clastic unit that is somewhat similar to the Tintic Quartzite in Rock Canyon. It is predominantly a quartz sand deposit like the Tintic and is overlain by a shale unit. The Flathead has a great variation in grain size from bottom to top and has a different vertical succession of primary sedimentary structures. Using the same criteria for the interpretation of

DUOLBASGAISSA FORMATION

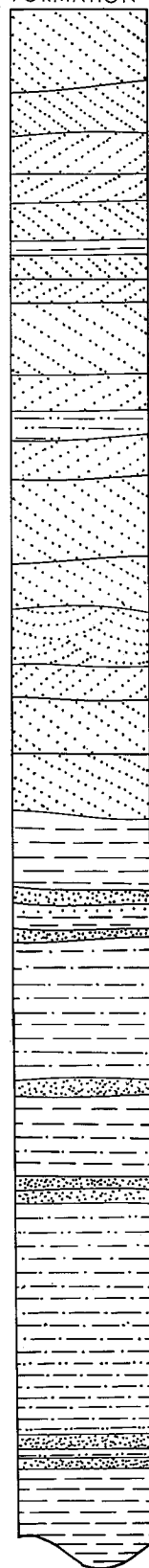


FIGURE 10.—Vertical succession of sedimentary structures in the Duolbasgaissa Formation of Norway. Not shown are abundant trace fossils throughout section. Total thickness, 550 m.

these structures as for the Tintic, the Flathead records a steady transition from high-energy surf conditions that worked very coarse conglomerates and sand in shallow water, to lower-velocity conditions in which fine-grained, well-differentiated sediment was transported by the migration of relatively straight-crested sandwaves.

These two formations are in sharp contrast to other rock units interpreted as tidal-flat deposits, such as the Duolbasgaissa Formation of northern Norway. This formation has mudstones and siltstones in the lower half in contrast to the conglomerates and coarse sands of the lower Tintic Quartzite and the Flathead Sandstone. In the upper half are quartzose sandstones with very large trough cross-bedding.

The model proposed here is an idealized vertical sequence of primary sedimentary structures and rock types for a transgressive, marine, clastic unit that is largely derived from studies of the Tintic Quartzite in the Wasatch Mountains. It postulates two main types of deposition. At the base is a conglomeratic unit, made up of immature sediments, that reflects initial deposition during transgression in high-energy surf conditions. Overlying this will be a body of sediment that will show an upward decrease in grain size and increasing maturity both compositionally and texturally, and the sedimentary structures will reflect decreasing current velocity and steadier current directions.

REFERENCES CITED

- Banks, N. L., 1973, Tide-dominated off-shore sedimentation, lower Cambrian, north Norway: *Sedimentology*, v. 20, p. 213-28.
- Curry, J. R., 1956, Analysis of two-dimensional orientation data: *Journal of Geology*, v. 64, p. 117-31.
- Eardley, A. J., 1944, Geology of the north-central Wasatch Mountains: *Geological Society of America Bulletin*, v. 55, p. 819-94.
- Eardley, A. J., and Harch, R. A., 1940, Proterozoic rocks in Utah: *Geological Society of America Bulletin*, v. 51, p. 795-844.
- Guy, H. P., Simons, D. B., and Richardson, E. V., 1966, Summary of alluvial channel data from flume experiments, 1956-1961: U.S. Geological Survey Professional Paper 462-I, 96p.
- Gwynn, T. A., 1948, Geology of Provo Slate Canyon in the southern Wasatch Mountains: Master's thesis, Brigham Young University, Provo, Utah.
- Hall, C. D., 1975, Petrography and cross-bedding analysis of the Flathead Sandstone, Teton County, Wyoming: In *Idaho Academy of Science Abstracts for 1975*.
- Hamblin, W. K., 1961, Paleogeographic evolution of the Lake Superior Region from Late Keweenaw to Late Cambrian time: *Geological Society of America Bulletin*, v. 72, p. 1-18.
- Hereford, R., 1977, Deposition of the Tapeats Sandstone (Cambrian) in central Arizona: *Geological Society of America Bulletin*, v. 88, p. 199-210.
- Irwin, M. L., 1965, General theory of epeiric clear-water sedimentation: *American Association of Petroleum Geologists Bulletin*, v. 49, p. 445-59.
- Ladle, G. H., 1972, The petrography and sedimentation of the Deadwood Formation in the Black Hills, South Dakota: National Aeronautics and Space Administration, MSC-06881, 179p.
- Liu, H. K., 1957, Mechanics of sediment-ripple formation: *American Society of Civil Engineers Proceedings*, v. 83, no. HY2, 23p.
- Lochman-Balk, C., 1959, The Cambrian section in the central and southern Wasatch Mountains: *Intermountain Association of Petroleum Geologists, Guidebook 10th Annual Field Conference, Geology of the Wasatch and Uinta Mountains transition area*, p. 40-45.
- _____, 1971, The Cambrian of the craton of the United States: In *Lower Paleozoic rocks of the world*, v. 1, Cambrian of the New World: Wiley-Interscience, London-New York.
- _____, 1972, Cambrian System-Geologic atlas of the Rocky Mountain region: *Rocky Mountain Association of Geologists*, p. 60-75.
- _____, 1976, The Cambrian Section of the central Wasatch Mountains: *Cordilleran Hingeline Symposium, Rocky Mountain Association of Geologists*, p. 103-108.

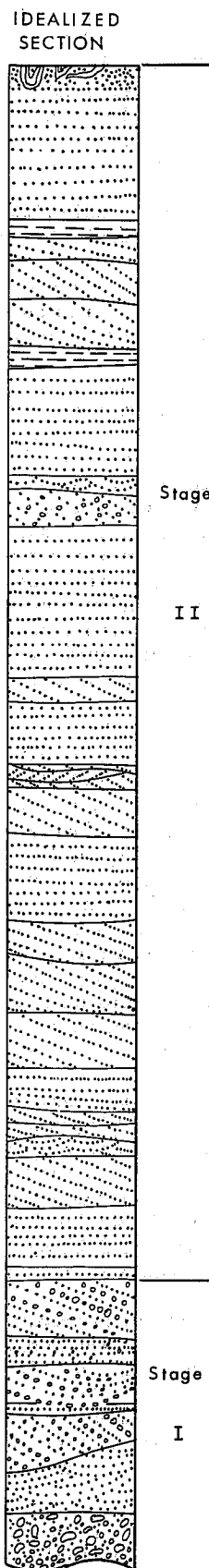


FIGURE 11.—Idealized vertical sequence of rock types and sedimentary structures deposited in a transgressive marine, shallow-water environment. It is applicable to siliciclastic sediments deposited in a high-energy, wave-generated current system.

- Maxey, G. B., 1958, Lower and middle Cambrian stratigraphy in northern Utah and southeastern Idaho: Geological Society of America Bulletin, v. 69, p. 647-88.
- Morris, H. T., and Lovering, T. S., 1961, Stratigraphy of the east Tintic Mountains, Utah: U.S. Geological Survey Professional Paper 361, p. 13-53.
- Oriel, S. S., and Armstrong, F. C., 1971, Uppermost Precambrian and Lowest Cambrian rocks in southeastern Idaho: U.S. Geological Survey Professional Paper 394, 52p.
- Pincus, H. J., 1956, Some vector and arithmetic operations on two-dimensional variates, with application to geologic data: Journal of Geology, v. 64, p. 533-37.
- Reineck, H. E., and Singh, I. B., 1975, Depositional sedimentary environments: Springer-Verlag, Berlin, 439p.
- Seeland, D. A., 1969, Paleocurrents in the basal clastic rocks of the Late Precambrian to Early Ordovician transgression of North America: In Abstracts for 1968: Geological Society of America Special Paper 121, p. 271-72.
- Smith, G. O., 1900, The Tintic district: U.S. Geological Survey Atlas Folio no. 65, 10p.
- Southard, J. B., 1971, Representation of bed configurations in depth-velocity-size diagrams: Journal of Sedimentary Petrology, v. 41, p. 903-15.
- Walter, J., 1894, Einleitung in die Geologie als Historische Wissenschaft: Bd. 3, Lithogenesis der Gegenwart, 535-1055, G. Fischer, Jena.

